



# Loop Current variability as trigger of coherent Gulf Stream transport

## anomalies

Joël J.-M. Hirschi\*

Eleanor Frajka-Williams

Adam T. Blaker

Bablu Sinha

Andrew Coward

*National Oceanography Centre, Southampton, SO14 3ZH, United Kingdom*

Pat Hyder

*UK Met Office, FitzRoy Road, Exeter, EX1 3PB*

Arne Biastoch

Claus Böning

*Helmholtz Centre for Ocean Research, Kiel, Germany*

Bernard Barnier

Thierry Penduff

16

Ixetl Garcia

17

*Université Grenoble Alpes, CNRS, IRD, Grenoble INP, IGE, Grenoble, France*

18

Filippa Fransner

19

*Geophysical Institute, University of Bergen and Bjerknes Centre for Climate Research, Bergen,*

20

*Norway*

21

Gurvan Madec

22

*LOCEAN (CNRS/IRD/UPMC/MNH) Institut Pierre et Simon Laplace, Paris, France*

23

*\*Corresponding author address:* National Oceanography Centre, Southampton, SO14 3ZH, United

24

Kingdom

25

E-mail: joel.hirschi@noc.ac.uk

## ABSTRACT

26 Satellite observations and output from a high resolution ocean model are  
27 used to investigate how the Loop Current in the Gulf of Mexico affects the  
28 Gulf Stream transport through Florida Straits. We find that the expansion  
29 (contraction) of the Loop Current leads to lower (higher) transports through  
30 the Straits of Florida. The associated surface velocity anomalies are coherent  
31 from the southwestern tip of Florida to Cape Hatteras. A simple continuity-  
32 based argument can be used to explain the link between the Loop Current  
33 and the downstream Gulf Stream transport: As the Loop Current lengthens  
34 (shortens) its path in the Gulf of Mexico the flow out of the Gulf decreases  
35 (increases). Anomalies in the surface velocity field are first seen to the south-  
36 west of Florida and within 4 weeks propagate through Florida Straits up to  
37 Cape Hatteras and into the Gulf Stream extension. In both the observations  
38 and the model this propagation can be seen as pulses in the surface velocities.  
39 We estimate that the Loop Current variability can be linked to a variability of  
40 several Sv ( $1\text{ Sv} = 10^6\text{ m}^3/\text{s}$ ) through the Florida Straits. The exact timing of  
41 the Loop Current variability is largely unpredictable beyond a few weeks and  
42 its variability is therefore likely a major contributor to the chaotic/intrinsic  
43 variability of the Gulf Stream. However, the time lag between the Loop Cur-  
44 rent and the flow downstream of the Gulf of Mexico means that if a length-  
45 ening/shortening of the Loop Current is observed this introduces some pre-  
46 dictability in the downstream flow for a few weeks.

## 47 **1. Introduction**

48 The Gulf Stream is a vigorous, warm surface western boundary current that forms the western  
49 branch of the Atlantic subtropical gyre. Its westward intensification is a direct consequence of  
50 the Earth's rotation and of the resulting Coriolis force. On a sphere the Coriolis force depends on  
51 the latitude (vanishing at the Equator; maximum at the poles) and it is this latitude dependence  
52 that leads to the westward intensified ocean circulation found along the western margins of the  
53 ocean basins (Stommel 1948). Of all western boundary currents the Gulf Stream is the best ob-  
54 served. In the Florida Straits it has been measured almost continuously since 1982 based on the  
55 voltage induced in submerged telecommunication cables (Larsen 1992; Baringer and Larsen 2001;  
56 DiNezio et al. 2009). On average the Gulf Stream transports about 31 Sv through the Florida Straits  
57 (Baringer and Larsen 2001; DiNezio et al. 2009). At Cape Hatteras the Gulf Stream separates from  
58 the US coast and flows eastward into the open Atlantic as the Gulf Stream Extension. Part of this  
59 current recirculates south in the upper ocean forming the eastern branch of the Subtropical Gyre  
60 and part of it flows northward towards the subpolar North Atlantic as the North Atlantic Current  
61 (NAC). The Gulf Stream constitutes a large fraction of the northward flowing surface branch of  
62 the Atlantic meridional overturning circulation (AMOC) (Cunningham et al. 2007, McCarthy et al.  
63 2012; Smeed et al. 2014).

64 As part of the AMOC the Gulf Stream affects climate and weather in the North Atlantic region  
65 and contributes to the net northward heat transport associated with the AMOC (e.g. Johns et al.  
66 2011). The cable measurements suggest that the Gulf Stream transport through Florida Straits  
67 has been largely stable during the last few decades. However, the transport is characterised by a  
68 large sub- to interannual variability. The majority of studies into the variability of the Gulf Stream  
69 transport have addressed the problem in terms of whether the temporal transport variability can

70 be explained as a response to variability in the atmospheric forcing (e.g. Anderson and Corry  
71 1985; DiNezio et al. 2009; Meinen et al. 2010; Atkinson et al. 2010; Sanchez-Franks et al. 2016).  
72 However, no approach can explain the full variability seen in the Gulf Stream transport. Arguments  
73 based on the wind stress/wind stress curl (e.g. Anderson and Corry 1985, Atkinson et al. 2010;  
74 Sanchez-Franks et al. 2016) argue that winds occurring either up or downstream of the Florida  
75 Straits are a main source of variability. However, it is also clear that the transport variability cannot  
76 be explained from the surface forcing alone. An example of this is the seasonal cycle seen in the  
77 Florida Straits transport (Niiler and Richardson 1973). The Florida Straits time series extending  
78 back to 1982 shows that this seasonal cycle is subject to a large interannual variability. In some  
79 years it is clearly defined, whereas during other years/periods the seasonal cycle is hardly visible.  
80 Seasonal variability in the large scale wind is thought to explain the seasonal cycle, but the wind  
81 has a seasonal cycle with comparatively little interannual variability and it is clear that factors  
82 other than wind determine the Gulf Stream variability on short i.e. subannual to annual time  
83 scales. In particular the Gulf Stream is subject to a large chaotic/intrinsic variability (Lin et al.  
84 2010; Atkinson et al. 2010; Mildner et al. 2013). Subjecting a model to the same atmospheric  
85 variability but starting from different initial conditions leads to different timings in the transports  
86 with low correlations between the different model realisations (Atkinson et al. 2010). The presence  
87 of chaotic (intrinsic) variability in the ocean has been studied before (e.g. Biastoch et al. 2008;  
88 Penduff et al. 2011; Hirschi et al. 2013; Grégorio et al. 2015; Leroux et al. 2018) but the emphasis  
89 of these studies was on variability of the sea surface height (SSH) or the AMOC and not on  
90 boundary currents. While the impact of the largely chaotic ocean eddies on the Gulf Stream  
91 transport is far from fully understood previous studies suggest that Loop Current eddies account  
92 for a sizeable fraction of the total variability in the Gulf Stream transport (Lin et al. 2010; Mildner  
93 et al. 2013) - in particular that certain stages of the Loop Current coincide with minima in the

94 volume transport through the Straits of Florida. The suggested mechanisms leading to reduced  
95 transport through the Florida Straits are either density and bottom pressure anomalies in response  
96 to an interaction between the Loop Current and the bottom topography between Florida and Cuba  
97 (Lin et al. 2010) or the partial blockage of transport through the Yucatan Channel (and hence at the  
98 outflow of the Gulf of Mexico through the Florida Straits) by Loop Current rings (Mildner et al.  
99 2013).

100 In this study we will show that there is a third, perhaps even simpler mechanism through which  
101 the Loop Current evolution can influence the variability of the volume transport through the Straits  
102 of Florida. Our results are based on a global high resolution ( $1/12^\circ$ ) ocean model and on satellite  
103 altimetry and concentrate on the coherent current made up of the Yucatan Current, the Loop  
104 Current, the Florida Current and the Gulf Stream. In the following we will refer to this “river-like”  
105 part of the current as the “Gulf Stream”. We show that variability on seasonal to interannual time  
106 scales exhibits a large spatial coherence along the US coastline and that the temporal evolution of  
107 the Loop Current is central to the variability found further downstream in the Straits of Florida and  
108 along the eastern US coast. We also show that the Loop Current is the trigger of pulses in the Gulf  
109 Stream transport which propagate from the Gulf of Mexico to Cape Hatteras in about 1 month.

## 110 **2. Data and Method**

111 The data used in this study consists of output from a high resolution global ocean model,  
112 geostrophic ocean surface velocities calculated from satellite altimetry and time series for the  
113 Gulf Stream transport obtained from cable measurements across the Florida Straits. For both  
114 the Florida Straits transport and surface velocities there are good quality observational data: the  
115 Florida Straits transport has been (almost) continuously observed since 1982 and surface velocities  
116 can be inferred from satellite altimetry since 1993. These quantities can also easily be compared

117 to results obtained in numerical ocean models (e.g. Marzocchi et al. 2015). The models then can  
118 be used to provide a more complete picture of the circulation as they can simulate the large scale  
119 three dimensional flow field at high resolution - something which cannot yet be obtained from  
120 observations.

121 The numerical model used in this study is the Nucleus for European Modelling of the Ocean  
122 (NEMO) (Madec 2008). NEMO simulates the global ocean circulation and uses the quasi-  
123 isotropic tripolar ORCA grid (Madec and Imbard 1996) with a horizontal resolution of  $1/12^\circ$ .  
124 To avoid a singularity at the North Pole the ORCA grid has two poles in the Northern Hemi-  
125 sphere centred on Northern Russia and Northern Canada respectively. Henceforth, we will refer  
126 to the numerical model as ORCA12. The atmospheric conditions needed to force the model are  
127 provided by version 4.1 of the DRAKKAR forcing dataset (DFS4.1, Brodeau et al. 2010). The  
128 ORCA12 simulation starts from rest and is initialised from the World Ocean Atlas 2005 clima-  
129 tological fields (Antonov et al. 2006; Locarnini et al. 2006) and covers the period from 1978  
130 to 2007 and has been shown to simulate a realistic circulation in the North Atlantic (Marzoc-  
131 chi et al. 2015; Blaker et al. 2015; Ducheze et al. 2014). Model output is available as 5-day  
132 averages. The observational data consists of geostrophic velocities computed from satellite al-  
133 timetry and are produced by Ssalto/Duacs and distributed by Aviso, with support from Cnes  
134 (<http://www.aviso.oceanobs.com/duacs>). The horizontal resolution of the geostrophic velocities  
135 is  $1/4^\circ$  and the data are available as weekly values. Here we use data from 1993 to 2010. The  
136 observation based estimates of the Gulf Stream transport cover the period from 1982 to present  
137 (Baringer and Larsen 2001; DiNezio et al. 2009; Meinen et al. 2010; Atkinson et al. 2010), but  
138 we use the period from 1993 to 2010. Gulf Stream transport data are available as daily mean val-  
139 ues from <http://www.aoml.noaa.gov/phod/floridacurrent/>. For the purpose of this study the Gulf  
140 Stream data are interpolated on the weekly time resolution of the AVISO data. There are missing

141 data for the Gulf Stream transport between 1998 and 2000 (funding gap) and September to Octo-  
142 ber 2004 (damage during the passage of Hurricanes Frances and Jeanne; DiNezio et al. 2009). A  
143 linear interpolation is used to fill the gaps in the Florida Straits transport data.

144 The cable based Florida Straits transport for the 1993 to 2010 period is 31 Sv with a standard  
145 deviation of 3 Sv (weekly averages). In the model the mean transport for the 1983 to 2007 period  
146 is also 31 Sv but the variability is weaker than in observations with a standard deviation of 2.1 Sv  
147 (5-day averages). For both the model and observational data we remove the long-term mean and  
148 unless stated otherwise we will use anomalies of velocity and transport in the remainder of the  
149 paper. Note that the accuracy of gridded satellite altimetry products near the coast has been ques-  
150 tioned (e.g. Cipollini et al. 2017) which could be an issue for our study given that the Gulf Stream  
151 hugs the US coast between Florida and Cape Hatteras. The use of a numerical model (ORCA12)  
152 for which the same limitation does not apply mitigates against this. However, any model inevitably  
153 has deficiencies in its ability to simulate the real world due to e.g. limited resolution or approx-  
154 imations in the physics. When identifying precursors/successors of transport anomalies in the  
155 Florida Straits we will therefore concentrate on features which are seen in ORCA12 as well as in  
156 the satellite observations as these are the features that are most likely to be robust.

157 For both the model and observational data we use composite analysis to illustrate links between  
158 the transport through Florida Straits and the large scale surface velocity field. Composites  $\Delta U^+$   
159 and  $\Delta U^-$  are computed for anomalies of the absolute surface velocities ( $U = \sqrt{u^2 + v^2}$ , where  
160  $u, v$  are the zonal and meridional velocity components) at the times  $t^+, t^-$  when the transport  
161 anomalies through Florida Straits are either positive or negative:



$$\Delta U^+(x, y) = \frac{1}{N^+} \sum_{i=1}^{N^+} \Delta U(x, y, t_i^+), \quad (1)$$

$$\Delta U^-(x, y) = \frac{1}{N^-} \sum_{i=1}^{N^-} \Delta U(x, y, t_i^-). \quad (2)$$

$N^+$  and  $N^-$  are the number of times when transport anomalies through the Florida Straits are positive or negative and  $\Delta U(x, y, t)$  are anomalies of the absolute surface velocity with respect to its long-term average  $\bar{U}$ :

$$\Delta U(x, y, t) = U(x, y, t) - \bar{U}, \quad \bar{U} = \frac{1}{t_s - t_e} \int_{t_s}^{t_e} U(x, y, t). \quad (3)$$

The start and end times  $t_s$  and  $t_e$  of the averaging period are 1993 and 2010 for the AVISO data and 1978 to 2007 for ORCA12. Unless stated otherwise no temporal filtering is applied to the model and satellite data. The composites  $\Delta U^+$  and  $\Delta U^-$  are computed using 5-day and weekly averages for the model and the observations, respectively. To understand how anomalies develop and in particular to identify circulation anomalies that either precede or follow volume transport anomalies through the Florida Straits we also compute lagged composites. Throughout this paper a negative lag means that surface velocities lead the transport variability through the Florida Straits and for a positive lag it is the variability in the Florida Straits transports which leads the anomalies seen in the surface velocity field.

### 3. Results

In the following we illustrate the spatial coherence of surface velocities associated with transport anomalies through the Florida Straits and propose a simple continuity-based explanation linking the Loop Current in the Gulf of Mexico to the Gulf Stream transport through Florida Straits.

178 *a. Spatial coherence*

179 The composites reveal striking coherence patterns (Figure 1) which are similar for both the  
180 ocean model and the observations. At zero lag the strongest coherent signal stretches from the  
181 southwest of Florida, to Cape Hatteras and into the Gulf Stream extension. Strong signals are  
182 also found in the Gulf of Mexico and to a lesser extent also in the Gulf Stream extension. The  
183 most obvious difference between the model and the observation based composites is the extent  
184 of the coherence patterns. Whereas the signal is largely confined between the Gulf of Mexico  
185 and the Gulf Stream extension in the observations, clear signals also occur further south in the  
186 model. This is particularly the case along the coast of South America between the Equator and  
187 about 15°N. These differences will not be further discussed here and in the following we will  
188 concentrate on the features that are common to both the model and the observations from the Gulf  
189 of Mexico to Cape Hatteras.

190 In the Gulf of Mexico the sign of the composite signal changes when moving downstream along  
191 the Gulf Stream path. For positive composites (i.e. absolute surface velocity patterns coinciding  
192 with positive transport anomalies in the Florida Straits) the positive velocity anomalies found along  
193 Florida change to negative values when moving upstream into the Gulf of Mexico. The negative  
194 anomaly in the Gulf of Mexico is loop shaped. This is most clearly seen in the observations. In  
195 the model the spatial shape is similar but the eastern flank of the loop shaped anomaly is less  
196 pronounced than in the observations. Interesting features are also seen north of Cape Hatteras in  
197 both the model and the observations. The composites suggest that positive (negative) Gulf Stream  
198 transport anomalies coincide with a southward (northward) shift of the Gulf Stream extension.  
199 In the model this can be seen most clearly just after the Gulf Stream detachment from the US  
200 coast. Between longitudes of about 75°W to 80°W the composite anomalies suggest a consistent

meridional shift of 1-2°. Moving further eastward the composite anomalies become weaker and less coherent but they still suggest that the meridional shift extends well into the Gulf Stream extension. In the observations the clear shift after Cape Hatteras is not seen, suggesting that it may be a numerical feature of the model. However, further east into the Gulf Stream extension there is a meridional shift of about 1-2° which extends to about 60°W. For positive transport anomalies through the Straits of Florida we find predominantly positive velocity anomalies in the southern part of the Gulf Stream extension which are flanked by negative velocity anomalies to the north. This picture is reversed for negative transport anomalies through the Florida Straits: Here the southern part of the Gulf Stream extension is characterised by predominantly negative velocity anomalies adjacent to positive velocity anomalies immediately to the north. The velocity anomaly patterns over the Gulf Stream extension region are consistent with small meridional shifts of the Gulf Stream extension. However, there are indications that the velocity anomalies indicative of a meridional shift in the Gulf Stream extension are not significant. Changing the time period over which the composites are computed, the meridional shift can be present (e.g. during the first half of the model integration) or absent (second half of integration, not shown). In the following analysis we will therefore concentrate on the strongest composite anomaly signal seen between the Gulf of Mexico and Cape Hatteras both in the observations and in the model. In the model the Florida Straits transport also exhibits an underlying long-term (decadal) variability with a gradual increase of 2-3 Sv until 1990 which is followed by a decrease by a similar amount after that. No longer term variability is evident in the cable observations of the Florida Straits transport.

To gain a dynamic picture of how the anomalies shown in Figure 1 evolve in time we look at lagged composites where Gulf Stream transport anomalies in the Florida Straits are related to the surface velocities either preceding or lagging them. In the model data we remove the long-term signal in the Florida Straits transport (red line in Figure 1) and only retain subannual to

interannual variability. We note that using the full variability does not change the basic links between the Loop Current and the Florida Straits transport we will describe below. However, removing the low frequency variability leads to clearer pictures and better agreement with the observations. The temporal behaviour of composite anomalies is most clearly seen in a movie (see supplementary material) but the main stages that have been identified are illustrated in Figures 2 and 3). The lagged composites show that clear surface velocity anomalies are seen in the Gulf of Mexico about 6 weeks before the Florida Straits transport anomaly. These velocity anomalies are largest in the region where Loop Current eddies are known to develop. These positive velocity anomalies in the central Gulf of Mexico coincide with the development of a negative velocity anomaly to the southwest of the southern tip of Florida. Within about two weeks this anomaly then rapidly extends eastward and along the coast of Florida, through the Florida Straits, and towards Cape Hatteras. From its starting point to the southwest of Florida to Cape Hatteras it takes about 40 days for the anomaly downstream of the Gulf of Mexico to reach its maximum expression. Beyond Cape Hatteras the anomaly field becomes too noisy to be tracked further into the Gulf Stream extension. In the satellite data (between lags of 0 and 15 days) there is a decrease of the velocity anomaly along the southern part of Florida whilst the anomaly increases off Cape Hatteras and into the Gulf Stream extension. In the model (between lags of 0 and 20 days) there is a decrease of the velocity anomalies everywhere from the Gulf of Mexico to Cape Hatteras. The velocity anomalies preceding and lagging the transport anomalies in the Florida Straits look like a “pulse” that rapidly propagates along the Gulf Stream flow. This pulse is somewhat reminiscent of the Natal pulses that occur in the Agulhas Current (Lutjeharms and Roberts 1988). However, as we will show next the mechanism is different here. Whereas Natal pulses are solitary meanders that result from anticyclonic eddies propagating along and interacting with the Agulhas current (Lutjeharms and Roberts 1988; de Ruijter et al. 1999; Leeuwen et al. 2000; Tsugawa and Hasumi

2010) the pulses described in this study are velocity anomalies (without any obvious meanders) which result from changes in the length of the Loop Current and the shedding of eddies.

*b. Loop Current length and downstream transport*

As mentioned earlier the composite anomalies that precede the appearance of the anomaly southwest of Florida are loop shaped (Figures 2 and 3). A striking feature is that the loop shaped anomaly in the Gulf of Mexico and the anomaly that propagates along the US coast are of opposite signs. To explain this feature we introduce a conceptual model (Figure 4). For simplicity we consider the Gulf Stream as a continuous river whose average path is indicated as a blue ribbon. During the formation of a Loop Current eddy (Figure 4a red ribbon) the length of the Loop Current path increases: rather than remaining confined to the eastern part of the Gulf of Mexico the Loop Current path extends well into the interior of the Gulf. As the Loop Current increases in length the water flowing into the Gulf of Mexico goes into lengthening the path. As a consequence the Gulf Stream transport at the outflow of the Gulf of Mexico will be reduced as the Loop Current expands. This reduction in transport will first be visible at the Gulf Stream outflow from where (consistent with Figures 2 and 3) it will then propagate along the coast of Florida, through Florida Straits and then further northwards towards Cape Hatteras. The opposite happens when a Loop Current eddy has been shed: The Loop Current path shortens (Figure 4b blue ribbon) and the Gulf Stream transport at the outflow of the Gulf of Mexico increases, triggering a positive velocity and transport anomaly which propagates towards Cape Hatteras. Note that the shedding of a Loop Current eddy is not necessary for there to be an imprint on the transport through Florida Straits. The Loop Current can also contract without an eddy being formed. Using this simple continuity argument the relationship between the flow through Florida Straits and the Loop Current length can be described as:

$$T_{FS} = T_{Yu} - A \frac{\partial L}{\partial t}, \quad (4)$$

where  $T_{Yu}$  and  $T_{FS}$  are the flow into (Yucatan Channel) and out of the Gulf of Mexico through the Florida Straits.  $A$  is the Gulf Stream cross section and  $L$  is the Gulf Stream length between Yucatan and the Florida Straits. For simplicity we assume  $T_{Yu}$  to be constant at 30 Sv and for  $A$  we assume the Gulf Stream width to be 50 km and its depth 500 m. Note that equation 4 assumes the flow out of the Gulf of Mexico to be a perfect indicator for  $T_{FS}$  and previous work has shown that this is not necessarily the case (Hamilton et al. 2005). However, as we will show later the variability of the flow out of the Gulf of Mexico can explain more than 60% of the variance in  $T_{FS}$  in our model.

To get an estimate of changes in  $T_{FS}$  linked to the Loop Current from equation 4 we assume the length of the Loop Current to vary by 500 km between the shortest and longest paths. For the purpose of illustration we assume a temporally sinusoidal lengthening and shortening of the Loop Current length i.e.  $L(t) = L_0 \cos(2\pi\omega t)$  and  $\omega = 1/\tau$  is varied for periods  $\tau$  between 1 year and 2 months and  $L_0 = 250$  km. The periods are chosen to cover the typical time scales for Loop Current eddy formation and shedding (one, occasionally two, Loop Current eddies are shed per year). Inserted into equation 4 this leads to:

$$T_{FS} = T_{Yu} + AL_0 2\pi\omega \sin(2\pi\omega t), \quad (5)$$

where  $AL_0\pi\omega$  is the amplitude of the transport variability in  $T_{FS}$ . According to equation 5 this expansion and contraction of the Loop Current length leads to transport anomalies of several Sv downstream of the idealised Loop Current. The higher the frequency  $\omega$  (generally: the faster the rate of length change) the larger the changes in Florida Straits transport  $T_{FS}$  become. For the

291 idealised values given above we find amplitudes of 1.2 Sv ( $\tau=1$  year) to 7.2 Sv ( $\tau=2$  months)  
 292 for  $T_{FS}$ . Note that expansion/contraction of the Loop Current length and transport anomalies are  
 293 not in phase. Transport anomalies reach maximum values when the rate of change in path length  
 294 reaches its maximum. In the simple example chosen here the time series of transport anomalies  
 295 is shifted by 90 degrees with respect to the path length. Obviously, the view presented above is  
 296 highly idealised: the Gulf Stream is not just an “oceanic river” with given width and depth that  
 297 occasionally sheds eddies. The Gulf Stream is a variable current with spatio-temporal changes in  
 298 both its width and depth. Nevertheless, it is between the inflow in Yucatan to Cape Hatteras that  
 299 the Gulf Stream is at its most coherent (Figure 1) and it is only when the Loop Current becomes  
 300 unstable whilst shedding Loop Current eddies that the flow cannot be identified as a coherent  
 301 flow band. This provides the motivation and some justification for the assumptions we make  
 302 here (Figure 4, equations 4, 5) and the simple considerations above suggest that the variability in  
 303 the Loop Current path length could be an important contributor to the variability of the transport  
 304 through Florida Straits. Note that the mass imbalance implied from equation 4 only applies to  
 305 the “river” through the Gulf of Mexico. An accumulation or deficit of volume transport into the  
 306 Gulf of Mexico would result in significant sea level change (about 5 cm/day for a imbalance of  
 307 1 Sv). Such changes are neither observed in the real ocean nor simulated in our model so any  
 308 imbalance occurring according to equation 4 will be largely compensated when considering not  
 309 just the “river” but the transports through the full sections between Yucatan and Cuba and between  
 310 Florida and Cuba. We will get back to this point later in this section.

311 In a next step we define a metric for the variability in the Gulf Stream length to establish whether  
 312 we can see an imprint of Loop Current length variability on the transport through Florida Straits in  
 313 the real North Atlantic and in ORCA12. We developed an algorithm which tracks the Gulf Stream  
 314 path by following the highest absolute surface velocity. With this “pathfinder” algorithm we can

determine the Gulf Stream path and length for each timestep (5-day averages for the model, weekly values for AVISO). The length of the Gulf Stream path is computed between the northeastern edge of the Yucatan Peninsula and the straits of Florida. The northeastern edge of Yucatan is where the Yucatan Current enters the Gulf of Mexico and both in the model and observations the strongest flow hugs the coast of Yucatan for most of the time. The starting point  $(x, y)_0$  of the path is where we find the highest velocity between Yucatan and Cuba when following the latitude of  $21.5^\circ\text{N}$  eastwards:

$$(x, y)_0 = \text{loc} \left[ \max \left( \sqrt{u^2(x, y_{21.5N}) + v^2(x, y_{21.5N})} \right) \right]. \quad (6)$$

Generally, the location  $(x, y)_0$  is found to be right at the coast of Yucatan. Starting from  $(x, y)_0$  the pathfinder algorithm follows the Gulf Stream path into the Gulf of Mexico and out through the Florida Straits up to Cape Hatteras by scanning the 8 neighbouring grid points. The decision from one step  $(x, y)_n$  to the next step  $(x, y)_{n+1}$  along the Gulf Stream path is based on both the amplitude of the current speed in the neighbouring cells as well as on the heading the flow has at point  $(x, y)_n$ . If  $i, j$  denote the grid coordinates of the path location  $(x, y)_n$  the next location  $(x, y)_{n+1}$  is found according to:

$$(x, y)_{n+1} = \text{loc} \left[ \max(w_{i,j+1}U_{i,j+1}, w_{i+1,j+1}U_{i+1,j+1}, w_{i+1,j}U_{i+1,j}, w_{i+1,j-1}U_{i+1,j-1} \right. \quad (7)$$

$$\left. w_{i,j-1}U_{i,j-1}, w_{i-1,j-1}U_{i-1,j-1}, w_{i-1,j}U_{i-1,j}, w_{i-1,j+1}U_{i-1,j+1}) \right], \quad (8)$$

where the values of the weights  $w$  depend on the heading of the flow at the location  $(x, y)_n$ . The weighting  $w$  is highest for the grid cells in the direction into which the velocity vector  $(u_n, v_n)$  is pointing. For a velocity vector consisting of positive northward and eastward components  $v$  and  $u$  the weights  $w$  are set to  $w = 20 + \sin(\alpha)$ ,  $w = 20 + \tan(\alpha)$ ,  $w = 20 + \cos(\alpha)$  for points  $(i, j+1)$ ,  $(i+1, j+1)$  and  $(i+1, j)$ , respectively, where  $\alpha$  is the angle between the velocity vector  $(u, v)$  and an eastward pointing vector. The weight is set to  $w = 6$  for the neighbouring points



335  $(i - 1, j)$  and  $(i + 1, j - 1)$  and  $w = 1$  for the remaining neighbours. Using much higher weights  
336 for the neighbours in the direction in which the flow is heading markedly reduces instances of the  
337 computed Gulf Stream path ending in a closed loop and the empirical values of 1, 6 and 20 were  
338 found to provide a faithful tracking of the maximum velocities along the Gulf Stream. Note that  
339 there can still be times when the Gulf Stream path ends up “trapped” in the Gulf of Mexico so that  
340 it never reaches the Florida Straits. This typically occurs when the Loop Current is in the process  
341 of shedding an eddy as during such periods the Gulf Stream flow between Yucatan and the Florida  
342 Straits no longer consists of a coherent stream. To avoid the path algorithm returning an undefined  
343 path the Gulf Stream path is set to the trajectory found for the last time step for which a valid  
344 path was returned i.e. a path which enters the Gulf of Mexico off northeastern Yucatan and exits it  
345 through the Florida Straits.

346 The density of Gulf Stream pathways inferred from satellite data and simulated by ORCA12  
347 are shown in Figure 5. Very similar probabilities are found for the simulated and observed Gulf  
348 Stream paths. When considering all paths, the highest probability is found for paths which extend  
349 well into the Gulf of Mexico. For both in the model and observations the highest probabilities  
350 indicate a loop which is oriented northwestwards and which is bound to the northeast by the West  
351 Florida Shelf and to the southeast by the Campeche Bank off the Yucatan Peninsula. The average  
352 length obtained when following the highest probabilities is about 1200 km. However, even though  
353 less likely, much shorter and longer paths also occur. The shortest ones (about 600 km in length)  
354 have hardly any incursion into the Gulf of Mexico and closely follow the northern coast of Cuba  
355 before entering the Florida Straits. The longest paths extend well into the Gulf of Mexico with  
356 lengths of 1500 km or more. Apart from a few exceptions all the Loop Current paths obtained  
357 in ORCA12 and in the observations are confined to the Abyssal Plain of the Gulf of Mexico. The  
358 highest density of paths occur to the northeast of Yucatan and along the east coast of Florida.

Both for the model and the observations every single path that can successfully be computed goes through Florida Straits. Between 24°N and 28°N in the Gulf of Mexico there is a slightly higher probability of long paths extending westward beyond 90W in the observations compared to ORCA12 suggesting that the model does not quite accurately represent the dynamics of the Loop Current. Another subtle difference between model and observations can be found along the coast of Florida north of about 30°N: Whereas all the paths computed in the model basically follow the same trajectory with only a gradual dispersion of paths when moving northwards, there are some paths peeling off into the basin interior in the observations. This suggests that the actual Gulf Stream along the US East Coast up to Cape Hatteras may be less stable than its modelled counterpart. Despite such differences the Gulf Stream path is well defined for most timesteps for the observational and for the model data.

To test whether the relationship between Florida Straits transport and Loop Current length proposed in equation 5 holds we select paths coinciding with either strong or weak transports. The threshold for selection is chosen as 1.5 times the standard deviation of the Florida Straits transport (Figure 5 middle and bottom panels). This threshold ensures that enough paths are retained for the probabilities whilst focussing on transports that are clearly stronger/weaker than the mean. We find a remarkable agreement between the model and the observations. Compared to the probabilities obtained using all paths there is a higher probability of short paths when only considering times when the transport is strong. The opposite holds true for weak transports and the highest probabilities are found for paths that extend well into the Gulf of Mexico. The link between path length and transports is weaker for positive than for negative transport anomalies. Even though the highest probabilities are found for short paths when transports are strong it is also clear that a strong Florida Straits transport can also coincide with intermediate and long paths. In comparison we find only few short paths coinciding with weak transports through the Florida Straits. There

383 is also a tendency for a more binary behaviour in this case with paths either being long or short  
384 with hardly any paths of intermediate length. Despite a range of path lengths being found to coin-  
385 cide with above or below average transport through the Florida Straits the results shown in Figure 5  
386 support the view that the length of Loop Current can be indicative of the transport strength through  
387 Florida Straits.

388 The close agreement between observations and the model motivates the use of the latter to  
389 further investigate how strongly Loop Current activity affects the transport through Florida Straits.  
390 The availability of the full 3-D velocity fields in the model means that transports in and out of  
391 the Gulf of Mexico can be studied in more detail (Figure 6). The conceptual model introduced  
392 in (5) assumes that between Yucatan and the Straits of Florida the Loop Current can be regarded  
393 as a “river”. This river is confined to the surface part of the ocean and the northward transport  
394 into the Gulf of Mexico occurs in the top 700 m. The 0-700 m depth range covers most of the  
395 cross section between Cuba and Florida and hence most of the net transport out of the Gulf of  
396 Mexico towards the Florida Straits. Relating transports between Yucatan and Cuba ( $T_{Yu}$ ) as well  
397 as between Cuba and Florida ( $T_{Cuba}$ ) to the Florida Straits transport ( $T_{FS}$ ) shows a markedly higher  
398 correlation between  $T_{Cuba}, T_{FS}$  ( $r=0.79$ , 62% explained variance) than between  $T_{Yu}, T_{FS}$  ( $r=0.59$ ,  
399 35% explained variance). Taking into account the transport in the top 700 m between Bahamas  
400 and Cuba ( $T_{Cuba-East}$ ) allows more than 90% of the variance of the Florida Straits transport to be  
401 recovered (correlation  $r(T_{Cuba} + T_{Cuba-East}, T_{FS}) = 0.95$ ). Looking at full depth transports for the  
402 same sections we get  $r(T_{Yu}, T_{Cuba}) = 1$ . Consistent with that the correlations  $r(T_{FS}, T_{Yu}) = 0.8$  and  
403  $r(T_{FS}, T_{Cuba}) = 0.81$  are almost identical. This means that (in the model at least) any mass storage  
404 term in the Gulf of Mexico linked to changes in the Loop Current length is negligible and that as  
405 we mentioned earlier there must be a compensation for the imbalance between the in- and outflow  
406 in the top 700 m. This compensation is captured when integrating transports over the full depths of

the sections between Yucatan and Cuba ( $B$ ) and between Cuba and Florida ( $C$ ). Considering full depth transports and assuming spatially uniform compensations through the channels the relation between the “river” transport into ( $T_{Yu}$ ) and out of ( $T_{Cuba}$ ) the Gulf of Mexico can be written as:

$$T_{Yu} + \frac{\beta A}{B} \frac{\partial L}{\partial t} \int_{x_1}^{x_2} dx \int_{-H_{Yu}}^0 dz + \frac{\gamma A}{C} \frac{\partial L}{\partial t} \int_{y_1}^{y_2} dy \int_{-H_{Cuba}}^0 dz - A \frac{\partial L}{\partial t} = T_{Cuba}, \quad (9)$$

where  $\beta + \gamma = 1$ . The integration limits  $x_1, x_2$  and  $y_1, y_2$  are the zonal and meridional end points of the Yucatan-Cuba ( $B$ ) and Cuba-Florida ( $C$ ) sections;  $H_{Yu}, H_{Cuba}$  are the maximum depths of the respective sections. The second to fourth terms on the left-hand side of equation 9 cancel each other out when integrating over the full cross sections. However, when considering the transports through the “river” cross section  $A$  these terms no longer compensate and equation 9 can be written as:

$$T_{Yu} + A^2 \frac{\partial L}{\partial t} \left( \frac{\beta}{B} + \frac{\gamma}{C} \right) - A \frac{\partial L}{\partial t} = T_{Cuba}, \quad (10)$$

In contrast to equation 4 equation 10 contains a compensation term (second left hand term) for the mass imbalance linked to the temporally changing length  $L$ . Only a fraction ( $A/B$  and  $A/C$ , respectively) of the compensations across sections  $B$  and  $C$  directly projects onto the “river” flow in and out of the Gulf of Mexico. Given the larger and deeper cross section area  $B$  between Yucatan and Cuba than between Cuba and Florida ( $C$ ) a larger fraction of the compensation is likely to flow through the former section (i.e.  $\beta > \gamma$ ). This is supported by the lower correlation we find between  $T_{Yu}$  and  $T_{FS}$  than between  $T_{Cuba}$  and  $T_{FS}$  (Figure 6). A compensation occurring mainly between Cuba and Florida is therefore unlikely. In the extreme case of all compensation occurring between Cuba and Florida (i.e.  $\beta = 0, \gamma = 1$ ) the correlations  $r(T_{Cuba}, T_{FS})$  and  $r(T_{Yu}, T_{FS})$  would have to be almost identical in the top 700 m as the top 700 m encompass most of the section between Cuba and Florida. However, the correlations presented in Figure 6 show that this is not the case. Identical correlations are only found when full depth transports are used across both sections.

428 *c. Timing of Loop Current and Florida Straits transport*

429 Having established that the variability in the Loop Current length is linked to the transport down-  
430 stream of the Gulf of Mexico, a natural question to ask is whether one can use the Loop Current  
431 length to predict transport anomalies through the Straits of Florida. The simple model in equations  
432 4, 5 suggests that there should be a phase shift of  $\pi/2$  between both time series. However, this  
433 rests on the assumptions that as the Loop Current expands or contracts its depth and width does not  
434 change, and that the length of the Loop Current varies periodically. This obviously doesn't have  
435 to be true meaning that even if Loop Current variations project onto the Florida Straits transport  
436 the phase relation between the Loop Current path length and the Florida Straits transport could  
437 change temporally. As a first step it is therefore useful to compare the spectra found in the tem-  
438 poral variability of the Florida Straits transport and of the Loop Current path length (Figure 7). A  
439 wavelet analysis shows that for both the variability of Florida Straits transports and of the Loop  
440 Current length most power is found for periods of 6 months or longer. This is the case in the model  
441 as well as in the observations. Cross-coherence is also strongest for periods of about 2-4 months  
442 or longer. Phases of significant cross-coherence occur for both the model and the observations.  
443 These phases are mainly confined to periods between 2 and about 6 years. There is indication of  
444 coherence on longer time scales but given the length of the time series confidence is low. The  
445 cross-coherence also shows that there is no consistent phase relationship between the Gulf Stream  
446 path variability and the Florida Straits transport. However, most phases of significant coherence  
447 have in common that the phase difference between the signals varies from about  $\pi$  (i.e. signal in  
448 antiphase phase, arrows pointing to the left) and about  $\pi \pm \pi/2$  (arrows still broadly pointing to  
449 left but with upwards/downwards component). This is broadly consistent with high/low transports  
450 through Florida Straits occurring during phases of short/long Loop Current length.

451 The cross-coherence can further be illustrated looking at the actual time series for Florida Straits  
452 transport and Loop Current length anomalies (Figure 8). The time series of the Gulf Stream path  
453 length and of the Florida Straits transport show that most peaks and troughs in transport have  
454 a counterpart in the Gulf Stream length (Figure 8). However, as shown in the wavelet cross-  
455 coherence analysis the phase shift between transports and path length for the simulated and ob-  
456 served Gulf Stream varies in time. There are times when the timeseries are mainly out-of phase  
457 (e.g. from 1983 to about 1990 in the model) or in phase (e.g. 2004 to 2006 in the observations)  
458 and there are also instances when the phase shift seems close to the  $\pi/2$  suggested in our simple  
459 conceptual model (e.g. 1997 to 1999 in observations or 2003 to 2004 in the model). Whereas the  
460 number of peaks and troughs in transport and path length suggests a link between Loop Current  
461 expansion and contraction and volume transport through Florida Straits, it is also clear that such a  
462 relationship can only partly be explained by the simple model based on continuity considerations  
463 as suggested in equations 4 and 5.

#### 464 **4. Discussion and conclusions**

465 Our results confirm earlier findings by Lin et al. 2010 and Mildner et al. 2013 who show that  
466 the evolution of the Loop Current can impact the Gulf Stream transport through Florida Straits.  
467 In these earlier studies the authors suggest that either interactions between the Loop Current and  
468 topography (Lin et al. 2010) or the presence of a ring north of Yucatan which reduces the flow  
469 into the Gulf of Mexico (Mildner et al. 2013) can lead to reductions in the volume transport  
470 through Florida Straits. Here, we have presented an additional view on how the Loop Current  
471 is likely to affect the flow downstream of the Gulf of Mexico. Using a simple continuity argument  
472 a lengthening/shortening of the length of the Loop Current should lead to a decrease/increase in  
473 the Gulf Stream transport downstream of the Loop Current. Our results suggest that the length-

474 ening/shortening of the Loop Current leads to pulses in the Gulf Stream transport which rapidly  
475 (within a few weeks) propagate from southern Florida to Cape Hatteras and which are triggered by  
476 expansion/contraction of the Loop Current. These pulses can be identified both in a high resolution  
477 ocean model as well as in observations of the real ocean (Figures 2, 3, supplementary material).  
478 The fact that we see these pulses both in the model and observations provides some confidence  
479 that we are looking at a robust signal and not just at an artefact of the model, or at a feature linked  
480 to limitations of satellite observations in coastal regions. Therefore, our results provide a strong  
481 indication that the Loop Current is likely to be a major contributor to the Gulf Stream variability  
482 further downstream along the coast of Florida and up to Cape Hatteras, in particular to its chaotic  
483 variability. Indeed, whereas the Loop Current is known to affect air-sea interactions (e.g. Putrasa-  
484 han et al. 2017), the actual timing of changes in the Loop Current is largely unpredictable from  
485 surface forcing (Oey et al. 2003; Oey et al. 2005) and results from baroclinic instability of the  
486 Loop Current (e.g. Donohue et al. 2016b), vorticity pulses from the Caribbean (Sheinbaum et al.  
487 2016), and/or coastally trapped waves originated within the Gulf of Mexico (Jouanno et al. 2016).  
488 As a consequence, movements of the Loop Current and the shedding of Loop Current eddies are  
489 largely chaotic (Donohue et al. 2016a).

490 Our study suggests that the expansion/contraction of the Loop Current can account for variations  
491 of several Sv in the Gulf Stream transport through Florida Straits on subannual time scales ((5),  
492 Figure 8). However, comparing time series of the Loop Current length and of the downstream  
493 volume transport also shows that the link between the two quantities is not as straightforward as  
494 in the simple model described by equation 4. For both the modelled and observed time series the  
495 lead-lag relation between the variability in Loop Current length and Florida Straits transport varies  
496 during the periods considered which means that the correlation between the two quantities is not  
497 high ( $r = -0.24$  for ORCA12 and  $r = 0.13$  for AVISO). It is also worth noting that there is also

no clear link between the amplitudes of the changes in path length and the transport variability. Nevertheless, even if not consistently aligned with the same lag, almost all peaks and troughs in the Gulf Stream transport through the Florida Straits have a counterpart in the variability of the Loop Current length. Together with the composite analysis showing the coherence and pulses of the Gulf Stream this supports the view that the waxing and waning of the Loop Current projects onto the Gulf Stream further downstream through Florida Straits and up to Cape Hatteras. At this point it is also worth reminding ourselves that particularly in the model, and to a lesser extent also in the observations there are downstream signals in the Caribbean Sea and along South America (Figure 1). These signals were not the focus of the present study but they may be indicative of precursors for the Loop Current variability.

The Gulf Stream is part of the wind-driven circulation. The action of the winds (via the wind stress) together with the Earth's rotation explain the strength and structure of the Gulf Stream. Being highly variable on all time scales winds are also a major source of variability for the Gulf Stream on subannual and longer time scales (Anderson and Corry 1985; DiNezio et al. 2009; Atkinson et al. 2010; Sanchez-Franks et al. 2016). However, these studies also show that variability in the wind stress is not sufficient to fully explain the variability in the western boundary current system comprising the Gulf Stream, the Yucatan Current and the Loop Current and a large fraction of the transport variability through Florida Straits has a different origin. In particular, to understand transport variability in the Gulf Stream through Florida Straits the intrinsic/chaotic variability of the ocean has to be taken into account as well. Our study supports the view that this chaotic ocean variability is likely to account for a large, possibly even the largest fraction of the Gulf Stream variability on sub- to interannual time scales. This chaotic variability in the ocean is linked to eddy and internal wave activity. In the case of the Gulf Stream eddies and waves can impact the transport as they approach the coast and start to interact with the western boundary



current system (e.g. Clément et al. 2016; Clément et al. 2014; Frajka-Williams et al. 2013, Kanzow et al. 2009; Zhai et al. 2010; Sinha et al. 2013, Hirschi et al. 2007). Alternatively western boundary currents can themselves produce eddies. In this case eddy formation starts as meanders in a coherent current which grow until they eventually break. This is seen e.g. in the Kuroshio and Gulf Stream extensions or as in this study in the Gulf of Mexico. It is these eddies that start as meanders that are at the heart of the ideas developed in Lin et al. (2010) and Mildner et al. (2013) as well as in the present study. Impacts of eddies on the temporal variability of the volume transport through Florida Straits are likely to have different origins. Such impacts can be linked to a local interaction of eddies with the current as they approach Bahamas from the basin interior (Frajka-Williams et al. 2013; Clément et al. 2014; Clément et al. 2016). However, it is also conceivable that eddies (or generally westward propagating features) reaching the coast further north could also affect the transport through Florida Straits. In this case perturbations could be mediated towards the Florida Straits as boundary trapped waves (e.g. Zhai et al. 2010; Sinha et al. 2013). To our knowledge such a situation has not yet been observed for the transport through Florida Straits. However, the concept of westward perturbations triggering equatorward, boundary trapped waves is well established in theory and in numerical modelling studies (e.g. Liu et al. 1999; van Sebille and van Leeuwen 2007; Kanzow et al. 2009) and in observations boundary waves have been shown to affect transports in the boundary currents in the Gulf of Mexico (Dubranna et al. 2011).

When considering the Loop Current there are several ways in which the Gulf Stream transport downstream could be affected via this current: (I) Increases or decreases of the flow into the Gulf of Mexico without changes in the path/shape of the Loop Current. This could for example occur when eddies in the Caribbean Sea propagate westwards towards northeastern Yucatan and attach to the Gulf Stream off Yucatan. In such cases anomalies through the Channel of Yucatan would essentially be passively advected along the Loop Current and into the Florida Straits. The transport

546 through the Yucatan Channel can also vary in response to large scale changes in the wind forcing  
547 over the region. (II) As the Loop Current expands, an anticyclonic eddy develops within the Loop  
548 Current which reduces the flow into the Gulf of Mexico by partly blocking the Yucatan Channel  
549 (Mildner et al. 2013). In this case the assumption is that the transport through Florida Straits is  
550 modulated by the flow into the Gulf of Mexico and that changes in the Loop Current length do  
551 not affect the outflow through Florida Straits. (III) In our study we propose a modulation of the  
552 Florida Straits transport as a response to the increase and decrease in length of the Loop Current  
553 based on a continuity argument along the current. In this case the transport through Florida Straits  
554 can change even if the inflow via the “river-like” Yucatan Current into the Gulf of Mexico is  
555 temporally constant. Note that as indicated by equation 9 and Figure 6 the full-depth transports  
556 across both sections *B* and *C* will be near identical at all times.

557 Whereas the mechanism proposed by Mildner et al. (2013) is consistent with a coherent trans-  
558 port/velocity anomaly between Yucatan and the Florida Straits (schematic in their figure 5) the  
559 mechanism we describe in the present study is consistent with the coherent transport/velocity  
560 anomalies which extend from southwest Florida to Cape Hatteras, something we find both in the  
561 model and the observations (Figures 1 -3). The mechanism as proposed by Mildner et al. (2013)  
562 can only be invoked to explain minima in the Florida Straits transports but does not provide an ex-  
563 planation for transport maxima. In contrast, the mechanism proposed here can be used to explain  
564 the development of both positive and negative transport anomalies. Our continuity-based mecha-  
565 nism presented here implies that at times there is a net inflow into or out of the Gulf of Mexico but  
566 the model suggests that this imbalance is compensated across the full depths of the Yucatan-Cuba  
567 and Cuba-Florida sections. To understand how and where such a compensation occurs would  
568 require the volume of the Loop Current to be computed as function of time and then linked to the  
569 flow through the sections *A* and *B*. Both the calculation of the Loop Current volume as a function

time and isolating the part of the cross section flow associated with these volume changes are far from trivial, however. An in-depth analysis of the exact nature and structure of the compensation is therefore left for a future study.

Nevertheless, equation 10 suggests that a barotropic compensation would be consistent with the relationships between the flow in and out of the Gulf of Mexico shown in Figure 6. However, it is likely that the compensation occurs as a consequence of processes of type (I), (II), and (III) working in concert. In particular the mechanisms proposed by Mildner et al. 2013 and Lin et al. (2010) and the mechanism proposed here are closely related. Part of the compensation required to e.g. compensate the net inflow as the Loop Current expands could follow the route south of Cuba suggested by Mildner et al. (2013) and the transport decrease through Florida Straits could be the consequence of both a reduced inflow into the Gulf of Mexico as well as to a reduction due to the expanding path length of the Loop Current. It seems plausible that mechanisms (I), (II) and (III) would typically work in combination rather than in isolation. This also means that the downstream impact of the Loop Current is hard (if not impossible) to quantify as processes (II) and (III) are difficult to separate. What is clear though is that both (II) and (III) can potentially account for transport anomalies of several Sv in the Florida Straits and therefore have the potential to explain a large fraction of the Florida Straits transport variability on subannual to perhaps interannual time scales. The chaotic nature of their timing means that they will also directly contribute to the intrinsic/chaotic variability in the Atlantic meridional overturning circulation as observed at 26.5°N (Smeed et al. 2014). What our study has also shown is that transport anomalies linked to the variability of the Loop Current are not confined to the Straits of Florida but extend all the way to Cape Hatteras where they may affect the Gulf Stream trajectory after its separation from North America and the stability of the flow in the Gulf Stream extension. This therefore suggests that there may be a direct link between the Loop Current activity and the Gulf Stream extension - an

594 area characterised by strong air-sea interactions and which is key to the cyclogenesis in the North  
595 Atlantic.

596

597 *Acknowledgments.* Constructive comments by two anonymous reviewers are gratefully ac-  
598 knowledged. JH, AB and BS acknowledge funding from the NERC project MESO-CLIP  
599 (NE/K005928/1) and from the NERC RAPID-AMOC project DYNAMOC (NE/M005097/1). AB,  
600 BS and AC also acknowledge funding from the NERC project ACSIS (NE/N018044/1). This work  
601 used the ARCHER UK National Supercomputing Service (<http://www.archer.ac.uk>) and is a con-  
602 tribution to the DRAKKAR project (<https://www.drakkar-ocean.eu>).

## 603 **References**

604 Anderson, D., and R. Corry, 1985: Ocean response to low frequency wind forcing with application  
605 to the seasonal variation in the Florida Straits-Gulf Stream transport. *Progress in Oceanography*,  
606 **14**, 7–40.

607 Antonov, J., R. Locarnini, T. Boyer, A. Mishonov, and H. Garcia, 2006: World Ocean Atlas  
608 2005, Volume 2: Salinity, NOAA Atlas NESDIS, vol. 62, edited by S. Levitus, pp 182, U.S.  
609 Government Printing Office, Washington. U.S. Government Printing Office, Washington.

610 Atkinson, C., H. Bryden, J. J.-M. Hirschi, and T. Kanzow, 2010: On the seasonal cycles and  
611 variability of Florida Straits, Ekman and Sverdrup transports at 26°N in the Atlantic Ocean.  
612 *Ocean Science*, **6** (4), 837–859.

613 Baringer, M. O., and J. C. Larsen, 2001: Sixteen years of Florida Current transport. *Geophys. Res.*  
614 *Let.*, **28**, 3179–3182.

- 615 Biastoch, A., C. W. Böning, and J. R. E. Lutjeharms, 2008: Agulhas leakage dynamics affects  
616 decadal variability in Atlantic overturning circulation. *Nature*, **456**, 489–492.
- 617 Blaker, A. T., J. J.-M. Hirschi, G. McCarthy, B. Sinha, S. Taws, R. Marsh, A. Coward, and  
618 B. de Cuevas, 2015: Historical analogues of the recent extreme minima observed in the At-  
619 lantic meridional overturning circulation at 26°N. *Climate Dynamics*, **44** (1-2), 457–473.
- 620 Brodeau, L., B. Barnier, A.-M. Treguier, T. Penduff, and S. Gulev, 2010: An ERA40-based atmo-  
621 spheric forcing for global ocean circulation models. *Ocean Modelling*, **31** (3), 88–104.
- 622 Cipollini, P., F. M. Calafat, S. Jevrejeva, A. Melet, and P. Prandi, 2017: Monitoring sea level in  
623 the coastal zone with satellite altimetry and tide gauges. *Surveys in Geophysics*, **38** (1), 33–57.
- 624 Clément, L., E. Frajka-Williams, K. Sheen, J. Brearley, and A. N. Garabato, 2016: Generation of  
625 internal waves by eddies impinging on the western boundary of the North Atlantic. *Journal of*  
626 *Physical Oceanography*, **46** (4), 1067–1079.
- 627 Clément, L., E. Frajka-Williams, Z. Szuts, and S. Cunningham, 2014: Vertical structure of eddies  
628 and Rossby waves, and their effect on the Atlantic meridional overturning circulation at 26.5N.  
629 *Journal of Geophysical Research: Oceans*, **119** (9), 6479–6498.
- 630 Cunningham, S. A., and Coauthors, 2007: Temporal variability of the Atlantic Meridional Over-  
631 turning Circulation at 26°N. *Science*, **317**, 935–938, doi:10.1126/science.1141304.
- 632 de Ruijter, W. P., P. J. Van Leeuwen, and J. R. Lutjeharms, 1999: Generation and evolution of Natal  
633 Pulses: solitary meanders in the Agulhas Current. *Journal of physical oceanography*, **29** (12),  
634 3043–3055.

- 635 DiNezio, P. N., L. J. Gramer, W. E. Johns, C. S. Meinen, and M. O. Baringer, 2009: Observed  
636 interannual variability of the Florida Current: Wind forcing and the North Atlantic Oscillation.  
637 *Journal of Physical Oceanography*, **39** (3), 721–736.
- 638 Donohue, K., D. Watts, P. Hamilton, R. Leben, M. Kennelly, and A. Lugo-Fernández, 2016a: Gulf  
639 of Mexico loop current path variability. *Dynamics of Atmospheres and Oceans*, **76**, 174–194.
- 640 Donohue, K. A., D. Watts, P. Hamilton, R. Leben, and M. Kennelly, 2016b: Loop current eddy  
641 formation and baroclinic instability. *Dynamics of Atmospheres and Oceans*, **76**, 195–216.
- 642 Dubranna, J., P. Pérez-Brunius, M. López, and J. Candela, 2011: Circulation over the continen-  
643 tal shelf of the western and southwestern Gulf of Mexico. *Journal of Geophysical Research:*  
644 *Oceans*, **116** (C8).
- 645 Duchez, A., E. Frajka-Williams, N. Castro, J. Hirschi, and A. Coward, 2014: Seasonal to in-  
646 terannual variability in density around the canary islands and their influence on the atlantic  
647 meridional overturning circulation at 26°N. *Journal of Geophysical Research: Oceans*, **119** (3),  
648 1843–1860.
- 649 Frajka-Williams, E., W. Johns, C. Meinen, L. Beal, and S. Cunningham, 2013: Eddy impacts on  
650 the Florida Current. *Geophysical Research Letters*, **40** (2), 349–353.
- 651 Grégorio, S., T. Penduff, G. Sérazin, J.-M. Molines, B. Barnier, and J. Hirschi, 2015: Intrinsic  
652 variability of the Atlantic meridional overturning circulation at interannual-to-multidecadal time  
653 scales. *Journal of Physical Oceanography*, **45** (7), 1929–1946.
- 654 Hamilton, P., J. C. Larsen, K. D. Leaman, T. N. Lee, and E. Waddell, 2005: Transports through  
655 the Straits of Florida. *Journal of Physical Oceanography*, **35** (3), 308–322.

656 Hirschi, J. J.-M., A. T. Blaker, B. Sinha, A. Coward, B. de Cuevas, S. Alderson, and G. Madec,  
 657 2013: Chaotic variability of the meridional overturning circulation on subannual to inter-  
 658 annual timescales. *Ocean Science*, **9** (5), 805–823, doi:10.5194/os-9-805-2013, URL [http:](http://www.ocean-sci.net/9/805/2013/)  
 659 [//www.ocean-sci.net/9/805/2013/](http://www.ocean-sci.net/9/805/2013/).

660 Hirschi, J. J.-M., P. D. Killworth, and J. R. Blundell, 2007: Subannual, seasonal and interannual  
 661 variability of the North Atlantic meridional overturning circulation. *J. Phys. Oceanogr.*, **37** (5),  
 662 1246–1265.

663 Johns, W. E., and Coauthors, 2011: Continuous, array-based estimates of Atlantic Ocean heat  
 664 transport at 26.5°N. *Journal of Climate*, **24** (10), 2429–2449.

665 Jouanno, J., J. Ochoa, E. Pallàs-Sanz, J. Sheinbaum, F. Andrade-Canto, J. Candela, and J.-M.  
 666 Molines, 2016: Loop Current frontal eddies: Formation along the Campeche Bank and impact  
 667 of coastally trapped waves. *Journal of Physical Oceanography*, **46** (11), 3339–3363.

668 Kanzow, T., H. L. Johnson, D. Marshall, S. A. Cunningham, J. J.-M. Hirschi, A. Mujahid, H. L.  
 669 Bryden, and W. E. Johns, 2009: Basin-wide integrated volume transports in an eddy-filled  
 670 ocean. *J. Phys. Oceanogr.*, **39**, 3091–3110.

671 Larsen, J., 1992: Transport and heat flux of the Florida current at 27°N derived from cross-stream  
 672 voltages and profiling data: Theory and observations. *Philosophical Transactions of the Royal*  
 673 *Society of London A: Mathematical, Physical and Engineering Sciences*, **338** (1650), 169–236.

674 Leeuwen, P. J., W. P. Ruijter, and J. R. Lutjeharms, 2000: Natal pulses and the formation of  
 675 Agulhas rings. *Journal of Geophysical Research: Oceans*, **105** (C3), 6425–6436.

676 Leroux, S., T. Penduff, L. Bessi eres, J.-M. Molines, J.-M. Brankart, G. S erazin, B. Barnier, and  
 677 L. Terray, 2018: Intrinsic and Atmospherically Forced Variability of the AMOC: Insights from  
 678 a Large-Ensemble Ocean Hindcast. *Journal of Climate*, **31** (3), 1183–1203.

679 Lin, Y., R. J. Greatbatch, and J. Sheng, 2010: The influence of Gulf of Mexico Loop Current  
 680 intrusion on the transport of the Florida Current. *Ocean Dynamics*, **60** (5), 1075–1084.

681 Liu, Z., L. Wu, and E. Bayler, 1999: Rossby wave–coastal Kelvin wave interaction in the extrat-  
 682 ropics. Part I: Low-frequency adjustment in a closed basin. *Journal of physical oceanography*,  
 683 **29** (9), 2382–2404.

684 Locarnini, R., A. Mishonov, J. Antonov, T. Boyer, H. Garcia, O. Baranova, M. Zweng, and  
 685 D. Johnson, 2006: World Ocean Atlas 2005, Volume 1: Temperature, NOAA Atlas NESDIS,  
 686 vol. 61, edited by S. Levitus, pp 182, U.S. Government Printing Office, Washington. U.S. Gov-  
 687 ernment Printing Office, Washington.

688 Lutjeharms, J., and H. Roberts, 1988: The Natal pulse: An extreme transient on the Agulhas  
 689 Current. *Journal of Geophysical Research: Oceans*, **93** (C1), 631–645.

690 Madec, G., 2008: Nemo ocean engine. Tech. rep., Institut Pierre-Simon Laplace (IPSL), France.  
 691 (Note du Pole de Mod elisation, 27), 300pp.

692 Madec, G., and M. Imbard, 1996: A global ocean mesh to overcome the North Pole singularity.  
 693 *Climate Dynamics*, **12** (6), 381–388.

694 Marzocchi, A., J. J.-M. Hirschi, N. P. Holliday, S. A. Cunningham, A. T. Blaker, and A. C. Coward,  
 695 2015: The North Atlantic subpolar circulation in an eddy-resolving global ocean model. *Journal*  
 696 *of Marine Systems*, **142**, 126–143.



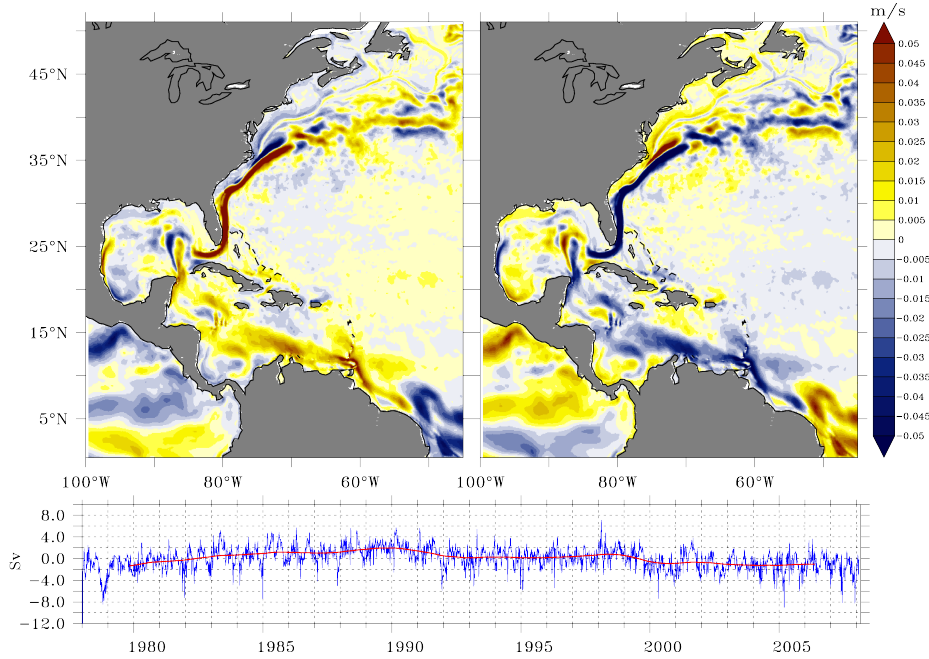
- 697 McCarthy, G., and Coauthors, 2012: Observed interannual variability of the Atlantic meridional  
698 overturning circulation at 26.5N. *Geophysical Research Letters*, **39** (19).
- 699 Meinen, C. S., M. O. Baringer, and R. F. Garcia, 2010: Florida Current transport variability:  
700 An analysis of annual and longer-period signals. *Deep Sea Research Part I: Oceanographic  
701 Research Papers*, **57** (7), 835–846.
- 702 Mildner, T. C., C. Eden, and L. Czeschel, 2013: Revisiting the relationship between Loop Cur-  
703 rent rings and Florida Current transport variability. *Journal of Geophysical Research: Oceans*,  
704 **118** (12), 6648–6657.
- 705 Niiler, P. P., and W. S. Richardson, 1973: Seasonal variability of the Florida Current. *J. Mar. Res.*,  
706 **31**, 144–167.
- 707 Oey, L.-Y., T. Ezer, and H.-C. Lee, 2005: Loop Current, rings and related circulation in the Gulf  
708 of Mexico: A review of numerical models and future challenges. *Circulation in the Gulf of  
709 Mexico: Observations and models*, 31–56.
- 710 Oey, L.-Y., H.-C. Lee, and W. J. Schmitz, 2003: Effects of winds and Caribbean eddies on the  
711 frequency of Loop Current eddy shedding: A numerical model study. *Journal of Geophysical  
712 Research: Oceans*, **108** (C10).
- 713 Penduff, T., M. Juza, W. K. Dewar, B. Barnier, J. Zika, A.-M. Treguier, J.-M. Molines, and N. Au-  
714 diffren, 2011: Sea-level expression of intrinsic and forced ocean variabilities at interannual  
715 timescales. *Journal of Climate*, **24**, 5652–5670.
- 716 Putrasahan, D., I. Kamenkovich, M. Le Hénaff, and B. Kirtman, 2017: Importance of ocean  
717 mesoscale variability for air-sea interactions in the Gulf of Mexico. *Geophysical Research Let-  
718 ters*.

- Sanchez-Franks, A., S. Hameed, and R. E. Wilson, 2016: The Icelandic Low as a predictor of the gulf stream north wall position. *Journal of Physical Oceanography*, **46** (3), 817–826.
- Sheinbaum, J., G. Athié, J. Candela, J. Ochoa, and A. Romero-Arteaga, 2016: Structure and variability of the Yucatan and loop currents along the slope and shelf break of the Yucatan channel and Campeche bank. *Dynamics of Atmospheres and Oceans*, **76**, 217–239.
- Sinha, B., B. Topliss, A. T. Blaker, and J.-M. Hirschi, 2013: A numerical model study of the effects of interannual time scale wave propagation on the predictability of the atlantic meridional overturning circulation. *Journal of Geophysical Research: Oceans*, (1), 131–146.
- Smeed, D., and Coauthors, 2014: Observed decline of the Atlantic meridional overturning circulation 2004-2012. *Ocean Science*, **10** (1), 29.
- Stommel, H., 1948: The westward intensification of wind-driven ocean currents. *Trans. Am. Geophys. Union*, **29**, 202–206.
- Tsugawa, M., and H. Hasumi, 2010: Generation and growth mechanism of the Natal Pulse. *Journal of Physical Oceanography*, **40** (7), 1597–1612.
- van Sebille, E., and P. J. van Leeuwen, 2007: Fast northward energy transfer in the Atlantic due to Agulhas rings. *Journal of Physical Oceanography*, **37** (9), 2305–2315.
- Zhai, X., H. L. Johnson, and D. P. Marshall, 2010: Significant sink of ocean-eddy energy near western boundaries. *Nature Geoscience*, **3** (9), 608.

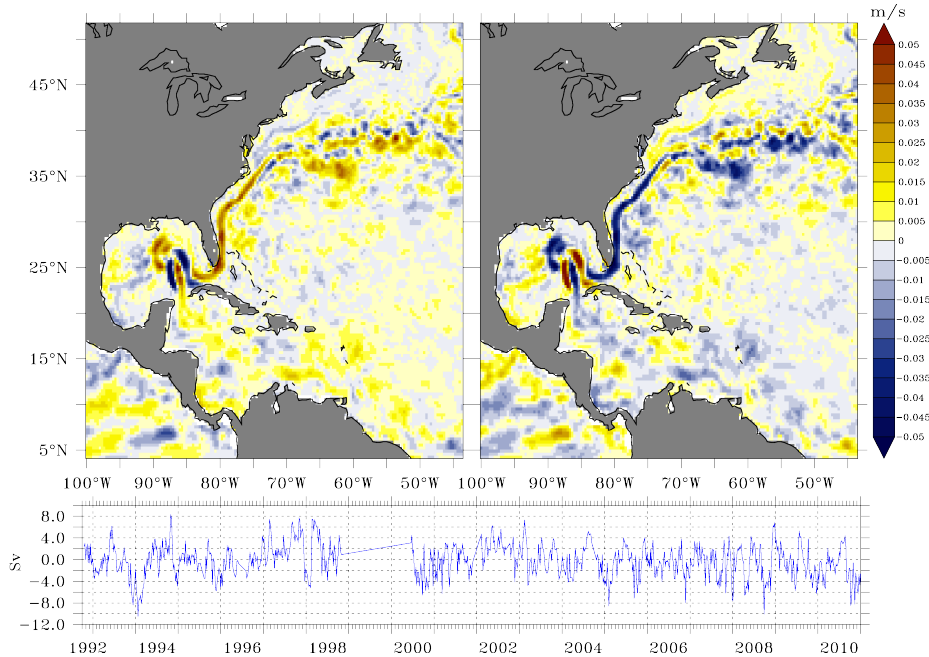
## LIST OF FIGURES

737			
738	<b>Fig. 1.</b>	a) Composites of absolute surface velocities for ORCA12. The positive and negative composites show the anomalous surface velocity pattern coinciding with the positive and negative transport anomalies in the Florida Straits shown in the bottom panel. The red line are the transport anomalies in the Florida Straits smoothed with a Parzen filter (window length of 1255 days). b) As a) but for geostrophic surface velocities inferred from AVISO. . . . .	35
739			
740			
741			
742			
743	<b>Fig. 2.</b>	Surface velocity anomalies in ORCA12 coinciding with negative transport anomalies through the Florida Straits at lags of (anticlockwise starting from top left panel) -40, -30, -15, 0, 20, and 110 days. Positive and negative lags indicate that transport anomalies in the Florida Straits are leading or lagging the surface velocity anomaly patterns in the Gulf of Mexico. Units are m/s. . . . .	36
744			
745			
746			
747			
748	<b>Fig. 3.</b>	Geostrophic surface velocity anomalies from AVISO coinciding with negative transport anomalies through the Florida Straits at lags of (anticlockwise starting from top left panel) -42, -28, -21, 0, 14, and 98 days. Units are m/s. . . . .	37
749			
750			
751	<b>Fig. 4.</b>	Schematic illustrating link between Loop Current eddy formation and Gulf Stream transport. . . . .	38
752	<b>Fig. 5.</b>	Gulf Stream path distributions for ORCA12 (left) and AVISO (right). Gulf Stream paths are computed for each weekly field between 1993 and 2010 for AVISO and for each 5-day average between 1983 and 2010 in ORCA12. The distributions show either all paths (top), for paths coinciding with Florida transports anomalies $> 1.5$ standard deviations (middle), and the distribution for paths coinciding with Florida Straits transports $< -1.5$ standard deviations. The green lines in the top left panels indicate the sections across which the transports shown in Figure 6 are computed. . . . .	39
753			
754			
755			
756			
757			
758			
759	<b>Fig. 6.</b>	Scatter plots and correlations for pairs of transports across the sections indicated in Figure 5. The transports used for the scatter plots and correlations are either computed for the top 700 m ( <b>top</b> ) or the full section depth ( <b>middle and bottom</b> ). . . . .	40
760			
761			
762	<b>Fig. 7.</b>	Top and middle rows: Wavelet analysis for Florida Straits transport and for time series of Loop Current length. Results are shown for ORCA12 (left) and AVISO (right). Bottom row: Wavelet cross coherence between Florida Straits transport and variability of Loop Current length. The units for the period are years and bold contours indicate when the timeseries for Florida Straits transport, the Loop Current length have statistically significant periodicities and when the coherence between both timeseries is statistically significant ( $p < 0.05$ ). Shading indicates either the wavelet power density or the coherency (both in arbitrary units). Arrows for the coherences indicate the phase between the timeseries. Arrows pointing to the right (left) indicate signals are in phase (out of phase). . . . .	41
763			
764			
765			
766			
767			
768			
769			
770			
771	<b>Fig. 8.</b>	Time series for anomalies of Gulf Stream transport (blue) and Loop Current length (red) for ORCA12 and AVISO. Units are Sv for the Florida Straits transport (left axis) and km for the path length (right axis). Time series for transports and path lengths have been high and low-pass filtered to only retain seasonal to interannual time scales where the strongest coherence is seen in Figure 7. The correlations between the Loop Current length and Florida Straits transport anomalies are -0.24 (ORCA12) and 0.13 (AVISO). . . . .	42
772			
773			
774			
775			
776			

a)



b)



777 FIG. 1. a) Composites of absolute surface velocities for ORCA12. The positive and negative composites  
 778 show the anomalous surface velocity pattern coinciding with the positive and negative transport anomalies in  
 779 the Florida Straits shown in the bottom panel. The red line are the transport anomalies in the Florida Straits  
 780 smoothed with a Parzen filter (window length of 1255 days). b) As a) but for geostrophic surface velocities  
 781 inferred from AVISO.

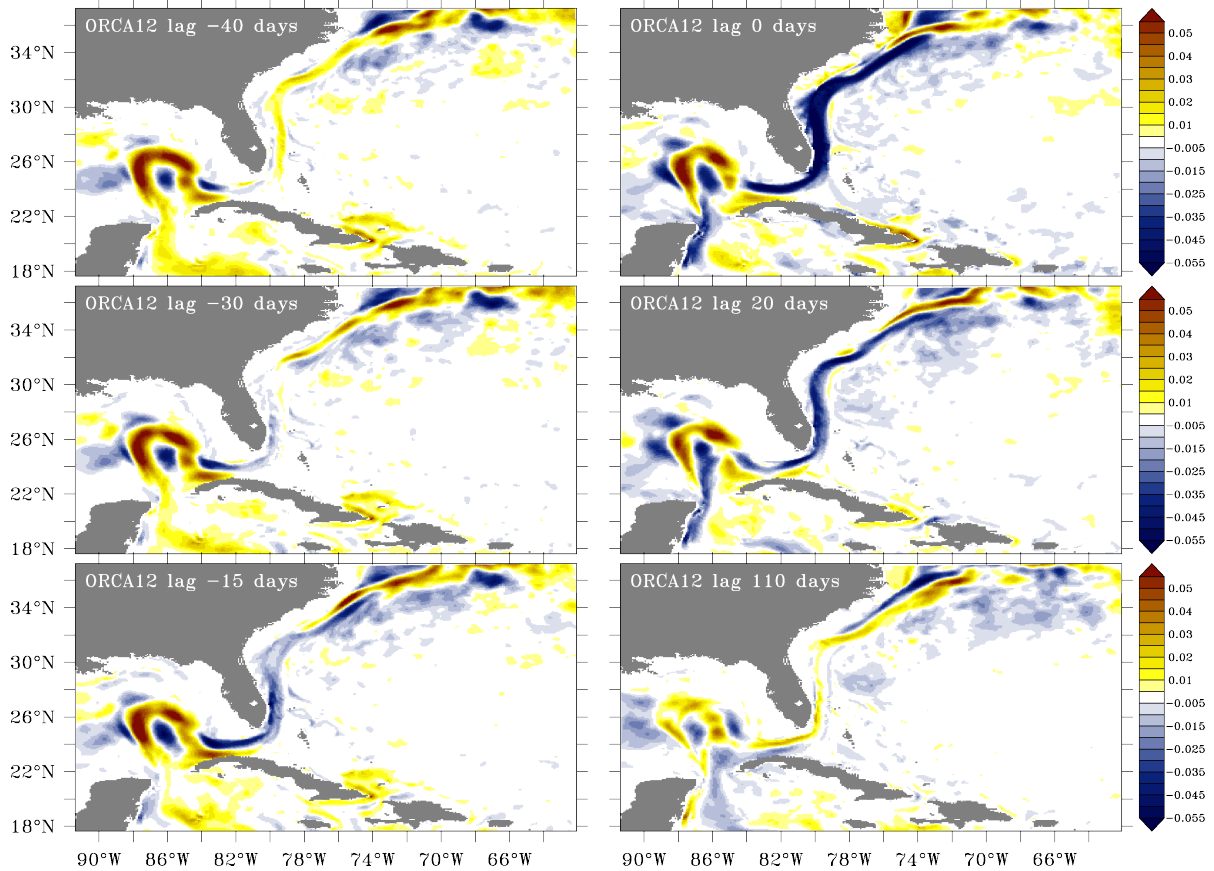


FIG. 2. Surface velocity anomalies in ORCA12 coinciding with negative transport anomalies through the Florida Straits at lags of (anticlockwise starting from top left panel) -40, -30, -15, 0, 20, and 110 days. Positive and negative lags indicate that transport anomalies in the Florida Straits are leading or lagging the surface velocity anomaly patterns in the Gulf of Mexico. Units are m/s.

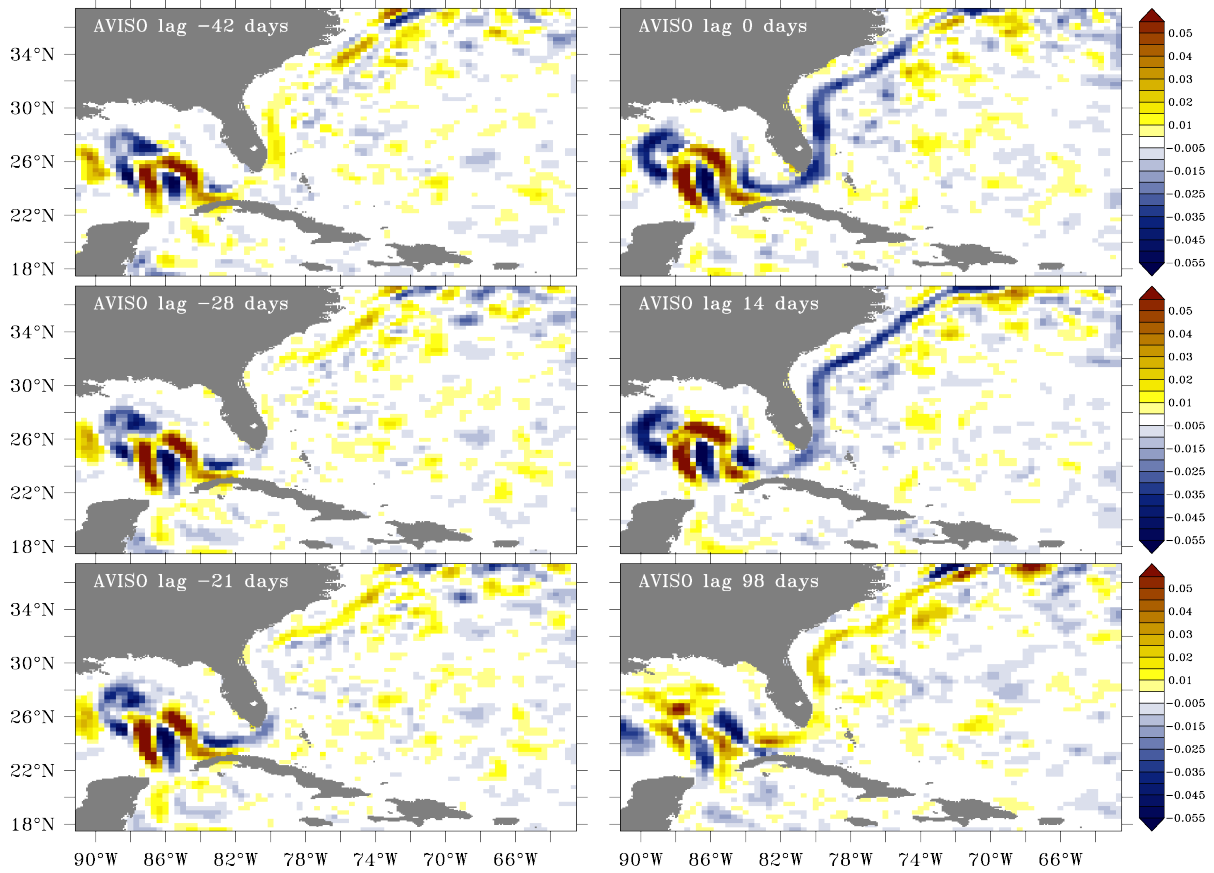
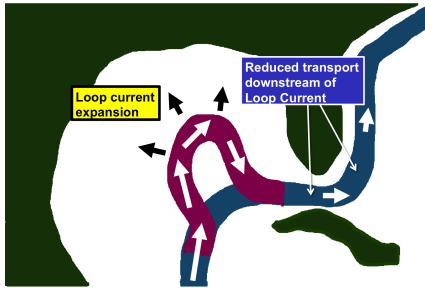


FIG. 3. Geostrophic surface velocity anomalies from AVISO coinciding with negative transport anomalies through the Florida Straits at lags of (anticlockwise starting from top left panel) -42, -28, -21, 0, 14, and 98 days.

Units are m/s.

a)



b)

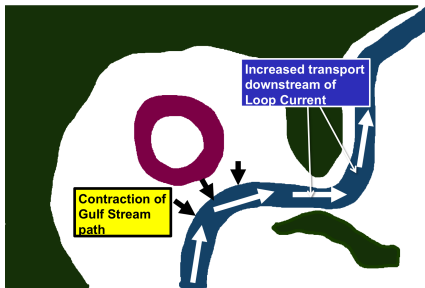


FIG. 4. Schematic illustrating link between Loop Current eddy formation and Gulf Stream transport.

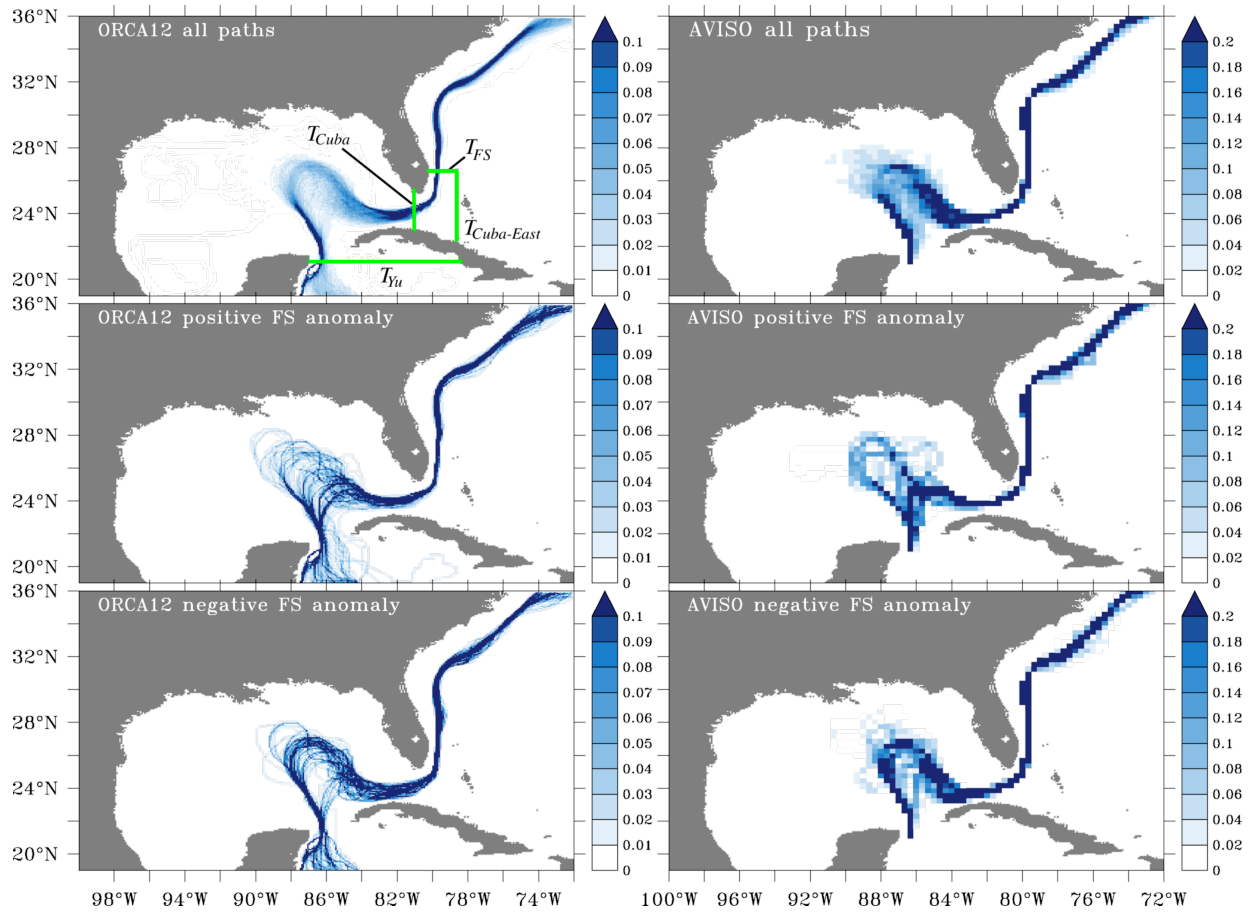


FIG. 5. Gulf Stream path distributions for ORCA12 (left) and AVISO (right). Gulf Stream paths are computed for each weekly field between 1993 and 2010 for AVISO and for each 5-day average between 1983 and 2010 in ORCA12. The distributions show either all paths (top), for paths coinciding with Florida transports anomalies  $> 1.5$  standard deviations (middle), and the distribution for paths coinciding with Florida Straits transports  $< -1.5$  standard deviations. The green lines in the top left panels indicate the sections across which the transports shown in Figure 6 are computed.



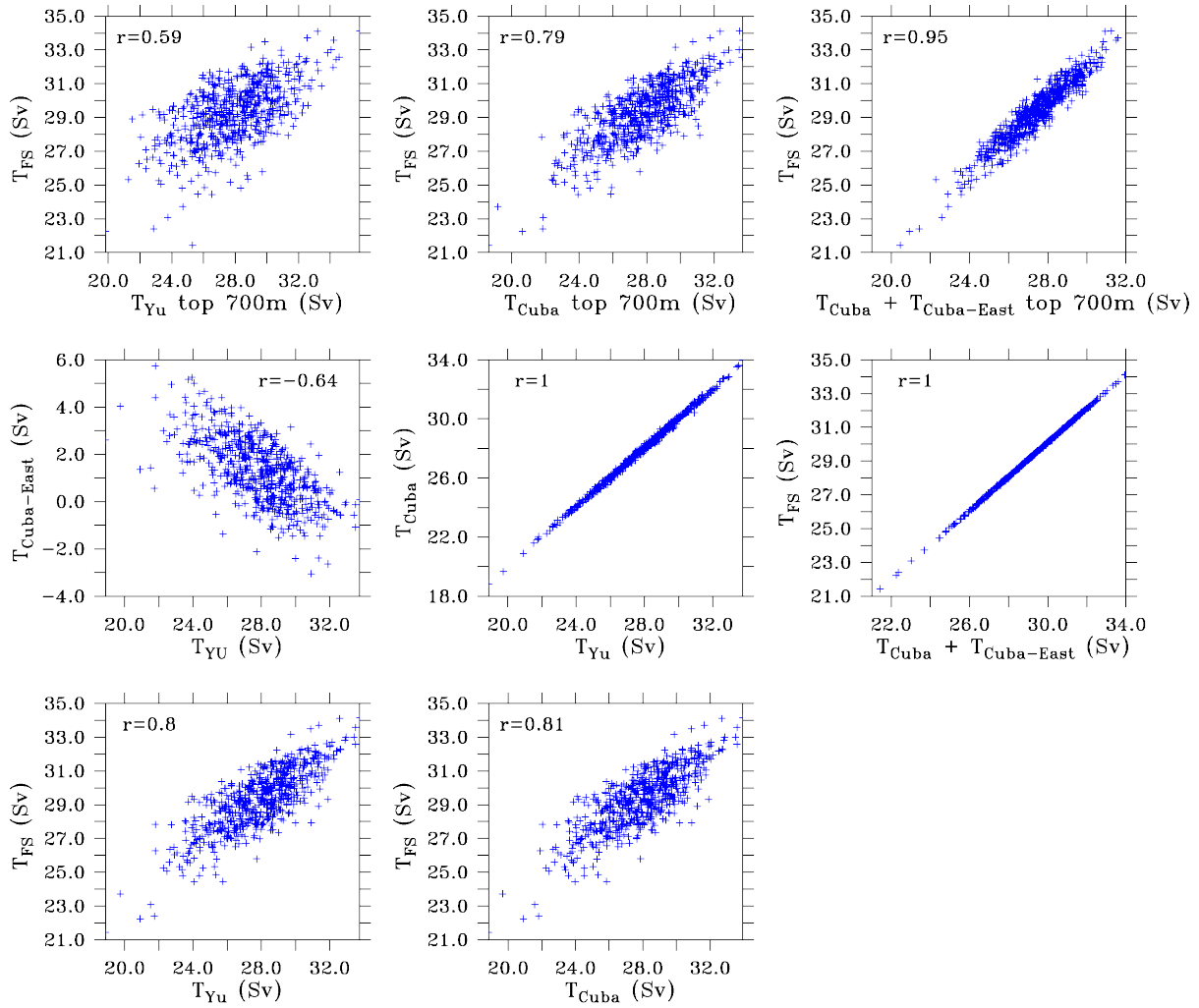
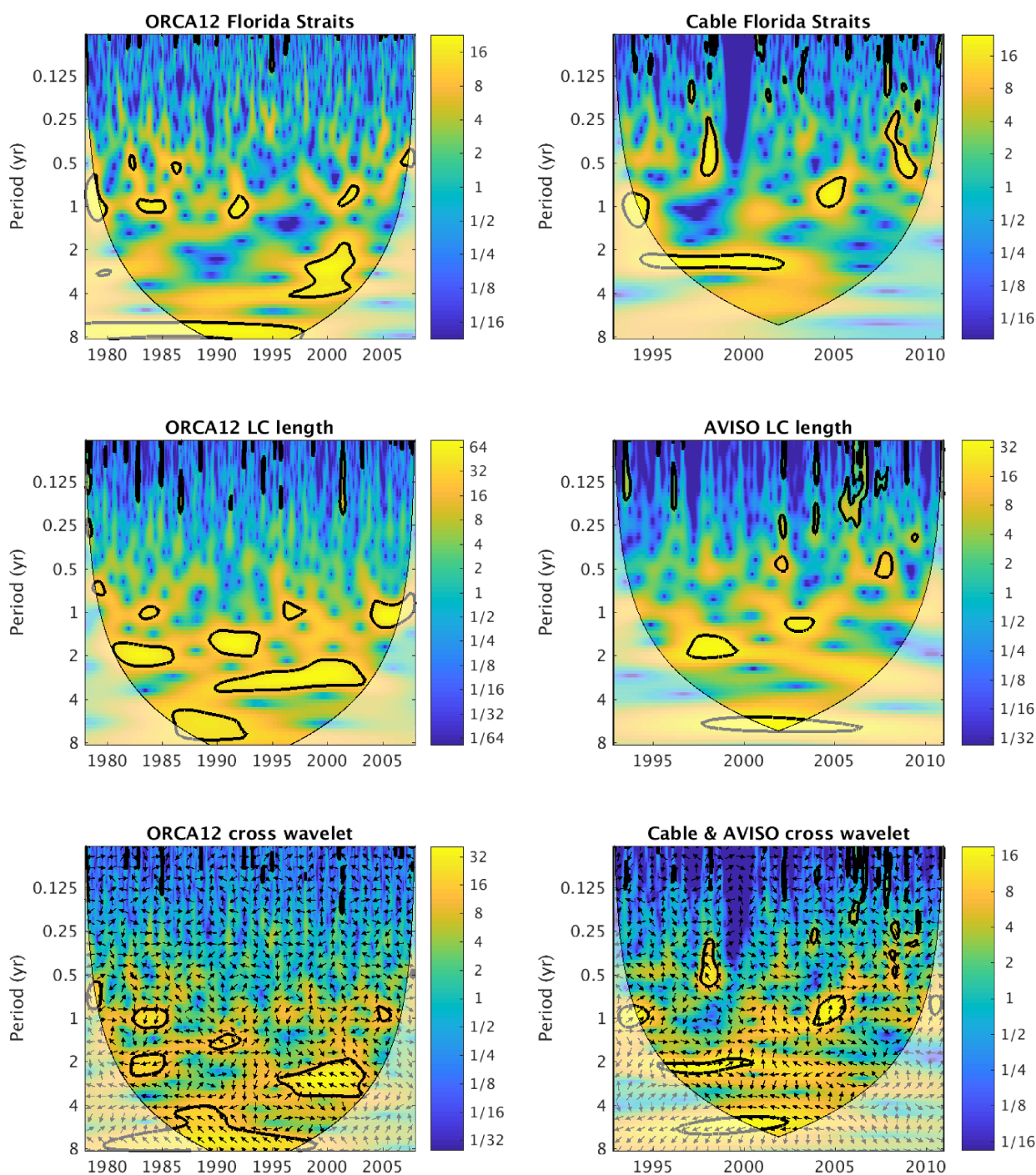


FIG. 6. Scatter plots and correlations for pairs of transports across the sections indicated in Figure 5. The transports used for the scatter plots and correlations are either computed for the top 700 m (**top**) or the full section depth (**middle and bottom**).



798 FIG. 7. Top and middle rows: Wavelet analysis for Florida Straits transport and for time series of Loop Current  
 799 length. Results are shown for ORCA12 (left) and AVISO (right). Bottom row: Wavelet cross coherence between  
 800 Florida Straits transport and variability of Loop Current length. The units for the period are years and bold  
 801 contours indicate when the timeseries for Florida Straits transport, the Loop Current length have statistically  
 802 significant periodicities and when the coherence between both timeseries is statistically significant ( $p < 0.05$ ).  
 803 Shading indicates either the wavelet power density or the coherency (both in arbitrary units). Arrows for the  
 804 coherences indicate the phase between the timeseries. Arrows pointing to the right (left) indicate signals are in  
 805 phase (out of phase).

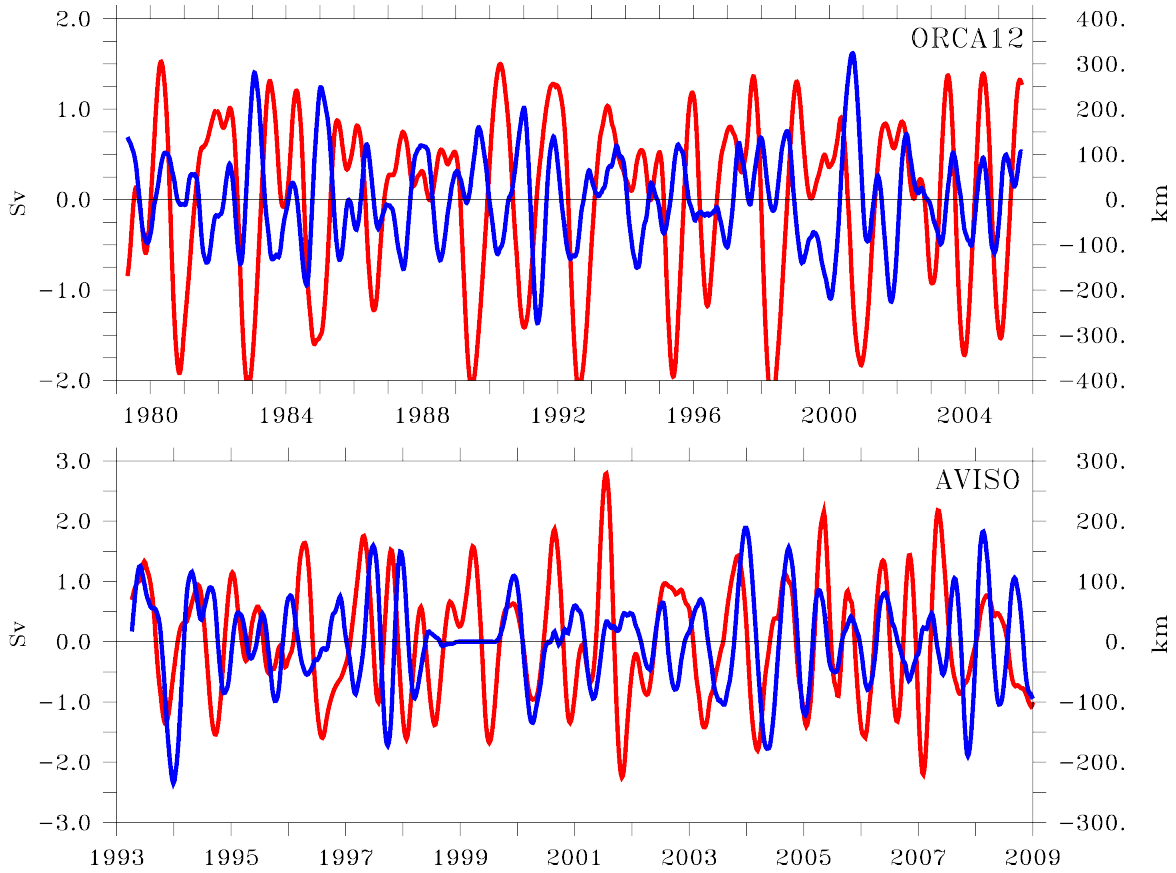


FIG. 8. Time series for anomalies of Gulf Stream transport (blue) and Loop Current length (red) for ORCA12 and AVISO. Units are Sv for the Florida Straits transport (left axis) and km for the path length (right axis). Time series for transports and path lengths have been high and low-pass filtered to only retain seasonal to interannual time scales where the strongest coherence is seen in Figure 7. The correlations between the Loop Current length and Florida Straits transport anomalies are -0.24 (ORCA12) and 0.13 (AVISO).